Comparative Mechanistic Studies on the Oxidation of Aromatic and Aliphatic Hydroxyl Derivatives in an Alkaline Medium at Preanodized Pt, Au and Pt/Au Electrodes in Presence of Redox Mediators

Sasha KALCHEVA[*] **, Philip IOTOV**
University of Chemical Technology and Metallurgy,
1756 Sofia, PO Box 32, BULGARIA

The role of redox mediators obtained from Pt, Au, and Pt/Au electrodes in the process of electro-catalytic oxidation of aromatic/aliphatic hydroxyl derivatives in an alkaline medium has been studied by applying cyclic voltammetry. Phenol and glycerol were used as aromatic and aliphatic hydroxyl derivatives in the electrochemical oxidation experiments. The results revealed that the presence of redox mediators formed by preliminary electrode anodization is crucial for the process of oxidation of aromatic compounds and imposes a different oxidation route for the aliphatic hydroxyl derivatives. The effect of preanodization has been related to the formation and dissolution of the corresponding higher hydrous oxides which accounts for the presence of M^{n+} in the solution. On subsequent positive scanning $M^{(n-x)+}$ -species are formed on the electrode surface thus increasing the active sites number. A tentative mechanism accounting for the oxidation process in the presence of redox mediators is suggested.

Introduction

The electrolytic strategies for the oxidative conversion of toxic organic pollutants has recently focused considerable research interest, as they offer versatility and environmental compatibility [1,2]. From thermodynamic viewpoint, all organic compounds are virtually degradable to CO_2 (mineralized) at potentials accessible at conventional electrodes. The observed deviation from this prediction is a consequence of kinetic rather than thermodynamic limitations. Therefore the current issue is to find out catalytic electrode materials which allow the occurrence of mineralization with high current efficiency.

DOC (Dissolved Organic Carbon) denotes the sum of dissolved degradable and non-biodegradable organic (aromatic) compounds in water. Due to the high toxicity of phenols and chlorophenols, efficient methods for their registration and control in waste waters are needed. One of the most perspective methods for the mineralization of phenolic compounds is the electrochemical treatment of effluent streams. This was evidenced by the contributions of Comninellis and De Battisti[3] on the anodic oxidation of phenol at

platinum and various DSA -anodes in aqueous alkaline solutions. It is well known that during the anodic treatment of aqueous phenolic solutions the formation of a passivating polymer film occurs at the electrode surface. In alkaline medium the polymerization product presents a polyoxi- phenylene (POP) film[4]. The formation of POP layer on the metal (Pt, Au, Ni, Ti, Cu, Fe, Zn, Cr) surface occurs, provided that the oxidation potential of the metal is greater than the discharge potential of the phenate anion (ArO^-). The POP film is resistant to acids and mineral bases, insoluble in water and alcohols but is soluble in aromatic solvents. An interesting fact is that water oxidation remains unaffected by the presence of phenols in aqueous media.

It is speculated that electrode fouling by adherent surface films is produced when the anodic mechanisms are unable to oxidize phenol beyond the state of simple free radicals, which determines the polymerization on the electrode surface. At the same time it is well known that the decrease of the anodic activity during the oxidation of organics at fixed potential before oxygen evolution can be overcome only at higher anode potentials with simultaneous O_2 evolution, which allows regeneration of the anodic surface. This was supported by a recent mechanistic study[5-6] of phenolic oxidation in acidic medium in the region of water discharge with simultaneous oxygen evolution. The results obtained ot Pt, Au and Pt/Au- alloy electrodes were rationalized on the basis of the Incipient Hydrous Oxide/Adatom Mediator (IHOAM) model of electrocatalysis. The behavior of gold electrode during the electrolysis of alkaline phenolic solutions was studied[7] as well. This material was selected due to the absence of unfavorable effects of surface blocking by adsorbed intermediate species. This excludes the appearance of inhibition effect observed at low potentials on Pt as Au is characterized by relatively weak adsorption properties[8,9] and high catalytic activity in alkaline medium[10].

Glycerol oxidation at various metals, metal alloys and adatom modified electrode surfaces was comparatively well studied[11-16]. There are no references on the oxidative transformation of glycerol and phenol at anodized electrode surfaces under comparative experimental conditions. The individual oxidative patterns of these hydrocarbons are to be compared with that obtained for their joint response. Besides, aliphatic intermediates like oxalic acid are formed during the later stages of the electrolytic oxidation of phenolic compounds. There are no literature data concerning the intermediates pointed above under the experimental conditions specified.

In this paper, we demonstrate novel experimental results on the oxidation of phenol and glycerol at preanodized Pt, Au and Pt/Au - alloy electrodes. These data are used to elucidate some mechanistic aspects of the process in an alkaline medium verifying the validity of the IHOAM model of electrocatalysis.

Experimental

The working electrodes were made of Pt, Pt/Au (40/60 at.%) alloy and Au plates with a geomteric area of 1 cm^2. Pt and Au counter electrode were used correspondingly.

Mercury / mercuric oxide reference electrode was used and for convenience all potential values were quoted vs. RHE. Fresh solutions of 'Merck' p.a. KOH were prepared directly from the solid. The base concentrations studied varied between 0.05 and 1M KOH. This corresponds to a pH range where the following water electrolysis intermediates: HO^{2-}, O^-, O^{2-} and O^{3-} are stable[17]. Phenol and glycerol were analytical grade produced by 'Chemapol' and 'Merck' respectively. The concentrations were varied from 10^{-4} to 10^{-1} mole l^{-1} for phenol and glycerol. All solutions were kept under nitrogen. The temperature was varied from 293.15 to 343.15 K. Nitrogen was purged through the solution in all cases between separate experiments.

In this study cyclic voltammetry was exclusively applied. The lower and upper potential limit were varied in each experiment in the range 0.02 to 3.25 V. The scan rate was 0.10 V s^{-1}. Hydrous oxides were grown through cycling[18-22] over various potential regions. The upper potential limit was varied to grow α- or β- oxides on the electrode surface, while the lower limit was fixed at a value providing the complete or partial preservation of the oxidative coverage at the electrode surface. The extent of surface oxidation was increased by varying the number of applied cycles, i.e. the polarization time.

Three separate procedures were applied for pretreatment of the working electrode if required:

(i) The surface oxide was removed from the electrode by using aqua regia;

(ii) The pretreatment in all cases of deposited POP film involved treating of the electrode surface with a fresh mixture of H_2O_2 (30 % aqueous solution) and $FeCl_3$ (5% aquoeus solution) at room temperature.

(iii) To ensure reproducibility of the electrode surface and activity, procedures (i) or (ii) were followed by pretreatment consisting in repetitive application of triangular potential sweeps with a rate of 0.10 V s^{-1} between oxygen and hydrogen evoluation potentials in the supporting electrolyte.

The true surface area of the electrode was determined prior to each experiment. Conventional procedures based on the estimation of charges required for H- coverage formation at Pt and the α_1- phase and for O - coverage removal at Au and the α_2- phase of the alloy electrode were used.

Results and Discussion

The potentiodynamic profile recorded for a given electroactive compound is suggested to be a function of thermodynamic, kinetic and diffusional parameters which characterize the occurring redox process. Its form is determined to a greater extent by the potential dependence of the electrode surface state than by the half potential of the hydrocarbon. When the electrode surface participates in catalytic processes the interpretatiton of potentiodynamic patterns is rather complicated.

Figures 1(a-c) show some complex responses for the prenodized Pt, Pt/Au- alloy and Au electrodes during the oxidative process of phenol. In accordance with the recent concepts the preanodization of noble metal electrodes[18-22] at potentials higher than 2 V, results in the formation of α- and β- oxides. As seen from Figure 1 (a and b), in presence of 10^{-4} M phenol the successive scanning leads to gradually increasing anodic and cathodic currents. This suggests that the oxides are partially removed and more favorable conditions for the subsequent oxidation process arise. This holds for Au under similar experimental conditions. For all studied electrode materials the anodic currents decrease on successive cycling at higher concentrations which is illustrated for Au in 10^{-2} M phenol in Figure 1 (c).

Figure 2 presents successive potentiodynamic profiles recorded in the potential range 0.70 to 2.50 V at preanodized Au. This figure is characterized by a gradual increase of the subsequent cathodic and anodic currents. The preliminary anodization of Au was carried in the same potential range and temperature. Figures 1 (c) and 2 refer to experiments carried out in solutions with equal phenolic concentration but with varying time of preliminary anodization. The following differences are observed:

- Both figures show reduction peaks at 0.77 V, but the one in Figure 2 is better outlined and its current density is considerably higher. According to literature data this peak is accounted by the presence of β- oxide on the electrode surface. The observed peak current density in Figure 2 increases with subsequent cycling probably due to the accumulation of a new chemical species.

- The anodic wave at 0.87 V in Figure 1 (c) is transformed into a well outlined peak in Figure 2. It is important to underline that this anodic peak is not observed during the first potential sweep, which is indicative for the absence of catalytic activity during the first scan. The peak current density increases with subsequent potential cycling.

The effect of preliminary anodization of the Pt, Pt/Au and Au electrodes on the electrooxidation of glycerol is illustrated in Figure 3 (a,b,c). The anodic currents recorded at Pt/Au -alloy and at Au electrode in aqueous solutions containing 0.1 M glycerol - Figure 3 (b and c) decrease on subsequent cycling. For all concentrations of glycerol studied, the oxide reduction at Pt- Figure 3 (a) is followed by an anodic current increase. In Figure 4 the reproducible potentiodynamic profiles of Pt, Pt/Au and Au obtained in the absence of preliminary anodization are displayed. In all three cases new anodic maxima are outlined at ca 2.5 V. This verifies that β- oxides grown under potentiodynamic conditions at all electrode materials used are catalytically active. The apparent contradiction between Figures 3 (a) and 4 (a) could be accounted to effect of oxygen evolution reaction (OER) on thick Pt- oxides films. It may be presumed that during the OER the porosity of thick oxide films is increased resulting in an enhanced rate of dissolution, which affects the amount of Pt ions in the solution and on the electrode surface. Some general points concerning the data in Figure 3 and 4 related to the catalytic oxidation of glycerol at preanodized surfaces are noteworthy:

- The observed anodic maximum in the absence of oxygen evolution [Figure 3 (a)] evidences the catalytic activity of Pt β- oxide on negative sweep at ca. 0.8 V. The low value of the peak current density is indicative of the occurrence of a surface chemical interaction. This assumption is supported by the form of the profile in the same potential range shown in Figure 4a. The higher Pt- oxide is consumed in the presence of the hydroperoxide anion obtained during oxygen reduction, which prevents glycerol oxidation.

- It is clear from Figure 3 (c) that the anodic process at preanodized Au electrode is initiated at ca. 0.7 V and proceeds at a considerably higher rate compared to Pt. On subsequent scanning the rate decreases due to the stepwise removal of Au β- oxide in this potential range. Data presented in Figure 4 (c) support the presumed catalytic activity of the Au β- oxide as a peak is observed at ca. 2.5 V in the absence of preliminary anodization. On negative sweep the β- oxide grown through potential cycling shows an oxidative activity towards glycerol.

- The observed behavior of the alloy electrode [Figures 3 (b), 4 (b)] may be interpreted on the ground of the explanations stated above.

The presence of thick oxide films on the surface of noble metal electrodes has a marked impact on the mechanism of electrode processes due to:

- Changes in the electronic properties of the electrode surface;

- Variation of the adsorption behavior of initial substrate and of intermediates at the anodized catalytic surface involving the site-blocking effect of the oxide functional group[22,23]. This effect depends on pH[24] of the solution, i.e. on the value of organic substrate/KOH ratio in the solution.
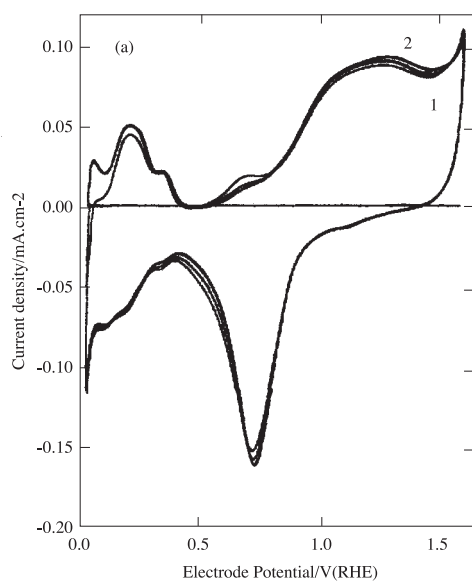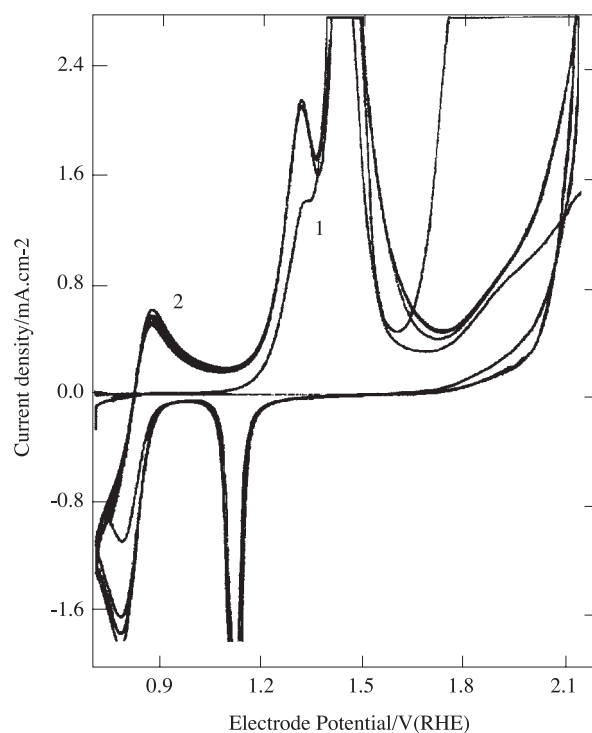
Figure 1a. Subsequent potentiodynamic profiles recorded at preanodized Pt in the potential range 0.02-1.55 V with a rate of 0.10 $V.s^{-1}$ at 308.15 K in a solution containing 0.3 M KOH and 10^{-4} M phenol: 1-first profile; 2-tenth profile. * The electrode surface oxides were grown for 750 s by preliminary cycling in the potential range 0.42-2.25 V with a rate of 0.10 $V.s^{-1}$ in 0.3 M KOH at 308.15 K.
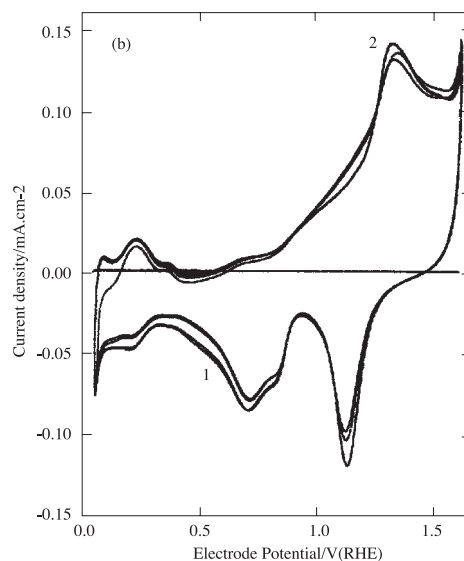
Figure 1b. Subsequent potentiodynamic profiles recorded at preanodized Pt/Au-alloy ($47.5\% \alpha_2$-phase) in the potential range 0.05-1.60 V with a rate of 0.10 $V.s^{-1}$ at 308.15 K in a solition containing 0.3 M KOH and 10^{-4} M phenol: 1-first profile; 2-tenth profile. * The electrode surface oxides were grown for 750 s by preliminary cycling in the potential range 0.40-2.25 V with a rate of 0.10 $V.s^{-1}$ in 0.3 M KOH at 308.15 K.
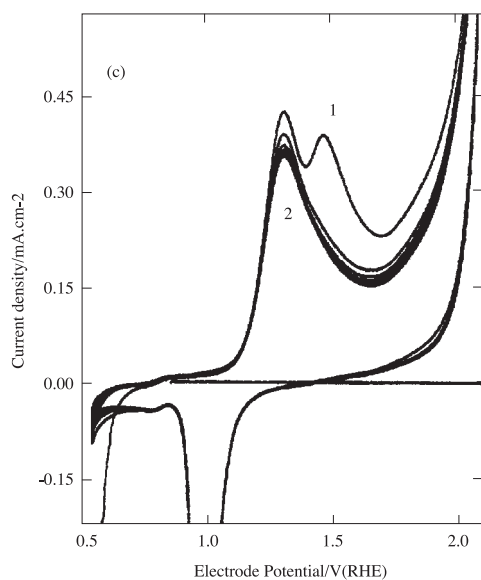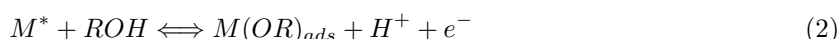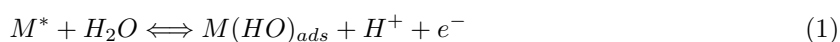

Figure 1c. Subsequent potentiodynamic profiles recorded at preanodized Au in the potential range 0.52-2.10 V with a rate of 0.10 $V.s^{-1}$ at 308.15 K in a solution containing 0.3 M KOH and 10^{-2} phenol: 1-first profile; 2-tenth profile. * The electrode surface oxides were grown for 240 s by preliminary cycling in the potential range 0.92-2.40 V with a rate of 0.10 $V.s^{-1}$ in 0.3 M KOH at 308.15 K.
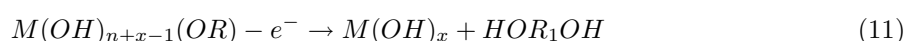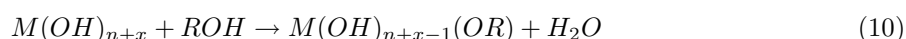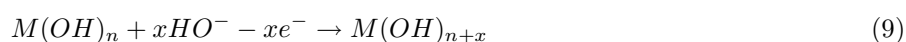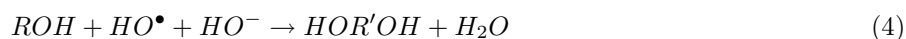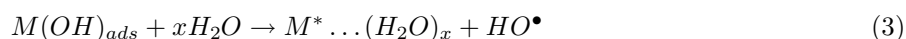
Figure 2. Subsequent potentiodynamic profiles recorded at preanodized Au in the potential range 0.70-2.50 V with a sweep rate 0.10 $V.s^{-1}$ at 342.65 K in a solution containing 0.3 M KOH and 10^{-2} M phenol: 1 -first profile; 2-tenth profile. * The electrode surface oxides were grown for 756s by preliminary cycling in the potential range 0.70-2.50 V with a sweep rate 0.10 $V.s^{-1}$ in 0.3 M KOH at 342.65 K.

The observed experimental results have clearly shown that the basic electrochemistry of noble metals is more complex than is generally assumed and a gap exists between theory and practice. To overcome this problem Burke et al.[25−31] have advanced the IHOAM model of electrocatalysis. They have proposed that the active interfacial mediators (adatoms and incipient hydrous oxide species) reside virtually outside the solid lattice and exhibit redox behavior very different to that of well embedded surface species. The main difference between this and the activated chemisorption model is that the adatom active sites are assumed to undergo a formal redox transition in the course of electrocatalysis. The IHOAM model states that when the organic material permeates through the porous oxide film being activated by coordination at the exposed adatoms sites, the removal of the thick film proceeds extremely rapidly. The effect of Au-adatoms deposition at Pt surface is demonstrated by the variation of the current -potential profiles during the catalytic oxidation of glycerol as displayed in Figure 5 (a). Au adatoms at Pt electrode surface resulted from the anodic dissolution of Au-oxides with the formation of Au ions, followed by anodization of Pt electrode in the same solution. The profiles recorded correspond to the responses observed at Pt/Au alloy electrodes which is an indirect evidence of the above assumption. It is additionally observed that the currents characterizing the presence of Au at the electrode surface decrease during subsequent cycling. Figure 5 (b) illustrates the effect of oxidation and reduction on the quantity of Au adatoms at Pt -electrode surface. Curve 1 corresponds to the Au modified Pt surface in the absence of organic substrate, while curve 2 refers to the first cycle after preliminary anodization aimed at Au- dissolution. It is seen that Au adatoms are dissolved during anodization and are deposited again on subsequent cycling. It is important to underline that these experiments were carried out to verify the partial dissolution of the surface oxide, resulting in
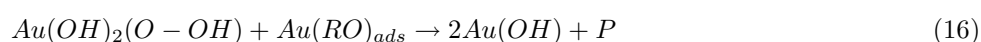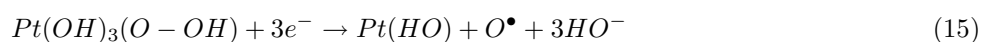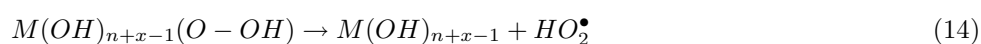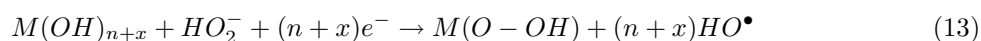
the formation of redox mediator couple. Similar observations were made in acidic media for Au at Pt by Cadle and Bruckenstein[32]. Data of Juodkazis et al.[33] have shown that the amount of Au^{3-} in HCl media is directly proportional to the amount of charge required for the reduction of anodically formed surface compounds. The foregoing results highlight that the IHOAM model of electrocatalysis is valid for oxidation of aromatic and aliphatic hydroxyl compounds in an alkaline medium at preanodized noble metal surfaces. A tentative unified mechanism is advanced to explain the experimental data obtained: On positive sweep the following reactions take place:
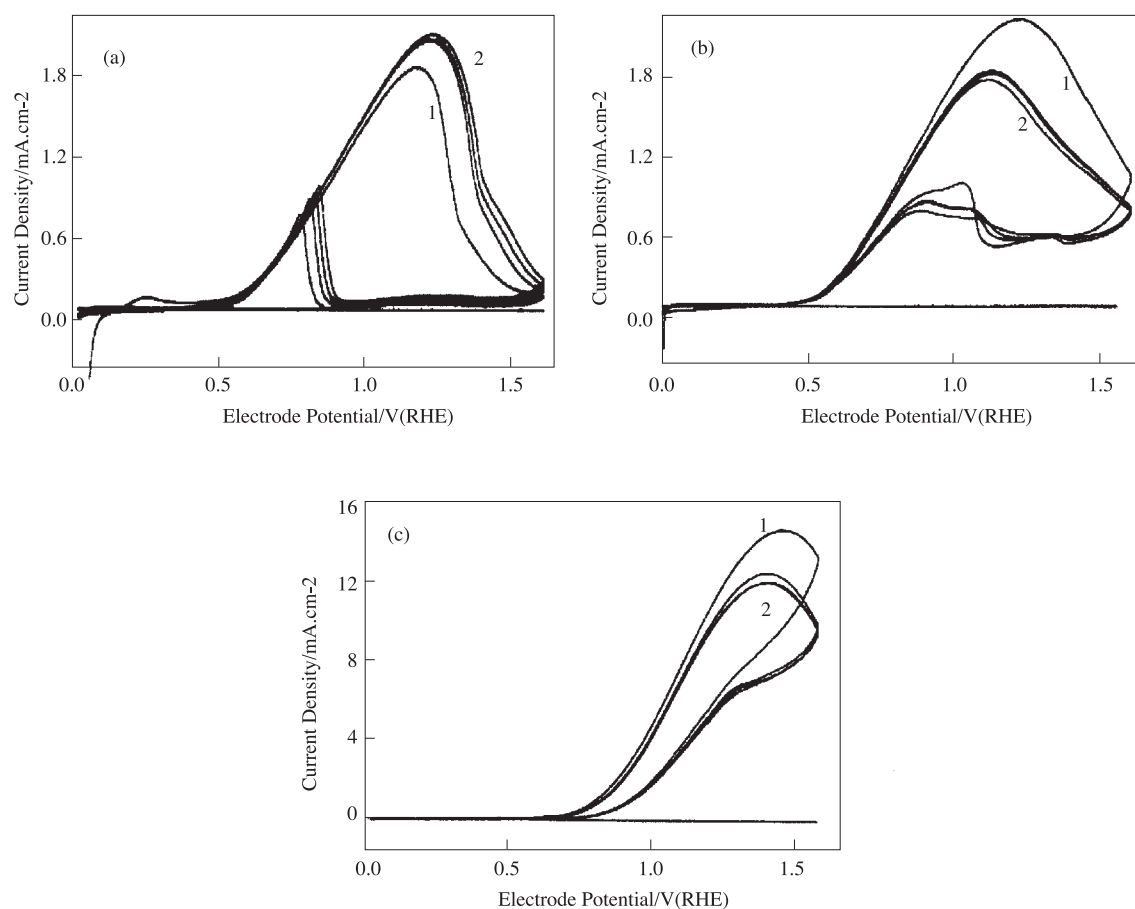
$$M^* + H_2O \Longleftrightarrow M(HO)_{ads} + H^+ + e^- \tag{1}$$

$$M^* + ROH \Longleftrightarrow M(OR)_{ads} + H^+ + e^- \tag{2}$$

where M^* denotes active noble adatoms; and R=C_6H_5-or $HOCH_2CH(OH)CH_2$-

$$M(OH)_{ads} + xH_2O \rightarrow M^* \ldots (H_2O)_x + HO^\bullet \tag{3}$$

$$ROH + HO^\bullet + HO^- \rightarrow HOR'OH + H_2O \tag{4}$$

$$M(OR)_{ads} + M(OH)_{ads} \rightarrow 2M^* + HOR'OH \ etc. \tag{5}$$

$$M(OR)_{ads} + H_2O \rightarrow M^* \ldots H_2O + RO^\bullet \tag{6}$$

$$nC_6H_5O^\bullet \rightarrow POP \tag{7}$$

$$M(OH)_{ads} + HO^- \rightarrow M(OH)_n + e^- \tag{8}$$

$$M(OH)_n + xHO^- - xe^- \rightarrow M(OH)_{n+x} \tag{9}$$

$$M(OH)_{n+x} + ROH \rightarrow M(OH)_{n+x-1}(OR) + H_2O \tag{10}$$

$$M(OH)_{n+x-1}(OR) - e^- \rightarrow M(OH)_x + HOR_1OH \tag{11}$$

where, n=2 and x=1, (Au) or x=2 (Pt); R is not equal to R_1 On negative sweep the following reactions occur:

$$O_2 + H_2O + e^- \Longleftrightarrow HO_2^- + HO^- \tag{12}$$

$$M(OH)_{n+x} + HO_2^- + (n+x)e^- \rightarrow M(O-OH) + (n+x)HO^\bullet \tag{13}$$

$$M(OH)_{n+x-1}(O-OH) \rightarrow M(OH)_{n+x-1} + HO_2^\bullet \tag{14}$$

$$Pt(OH)_3(O-OH) + 3e^- \rightarrow Pt(HO) + O^\bullet + 3HO^- \tag{15}$$

$$Au(OH)_2(O-OH) + Au(RO)_{ads} \rightarrow 2Au(OH) + P \tag{16}$$

$$M^* + HO_2^- \Longleftrightarrow M(OH) + O^\bullet \tag{17}$$

$$O^\bullet + M(RO)_{ads} \rightarrow M^* + P \tag{18}$$

where, P denotes a product;

Figure 3. Subsequent potentiodynamic profiles recorded in the range of 0.05-1.60 V.s^{-1} at 308.15 K in a solution containing 0.05 M KOH and 0.1 M glycerol: 1-first profile; 2-fourth profile. (a) Profiles recorded at oxides grown by preliminary cycling of Pt for 735 s in the range of 0.70-2.50 V with a rate of 0.10 V.s^{-1} in 0.05 M KOH at 308.15K. (b) Profiles recorded at mixed metal oxides grown by preliminary cycling of a Pt/Au-alloy (2.5% α_2-phase) electrode for 735 s in the range of 0.70-2.50 V with a rate of 0.10 V.s^{-1} in 0.05 M KOH at 308.15 K. (c) Profiles recorded at oxides grown by preliminary oxides of Au for 735 s in the range of 0.70-2.50 V with a rate of 0.10 V. s^{-1} in 0.05 M KOH at 308.15 K.

In absence of oxygen evolution, the process is initiated by the adsorption of the hydroxyl compounds at the active metal adatoms prior to 0.60 V, as illustrated by equations (1) and (2). Hydroxyl radicals are formed in accordance with equation (3). The anodic wave at ca 0.70 V (Figure 1) is assumed to be determined by a sequence of reactions (1)-(4). Reaction (5) presents a slow heterogeneous chemical step resulting in the formation of products, which are desorbed from the surface. It is noteworthy to mention that similar observations were made by Conway et al.[34] for the anodic oxidation of another sp-metal (Ag) in the presence of methanol. It was observed that the anodic oxidation of Ag in an acid medium proceeds with the successive formation of Ag_2O and AgO and that methanol was oxidized only at the surface of the first oxide. The results of Kotz and Yeager[35] who presented a photo electrochemical study of polycrystalline Ag in 1M KOH by using ex-situ Raman spectroscopy, confirm these data. Fleischmann et al.[36] have investigated the electrochemical behavior of phenol at Ag in an alkaline medium and their data presented supporting evidences. The radicals formed at potentials slightly above 0.7 V, eqs. (3) and (6) determine two types of anodic interactions described by equations (4) and (7). Reactions (8) and (9) present the growth of α

and β- oxides respectively. The catalytic effect of the surface β- oxide as seen from Figures 1 and 3. The interaction between higher valent oxide and the organic substrate is described by equations (10) and (11). The preanodized electrode surface behaves as a hydrous oxide - alloy electrode[37]. Oxygen reduction at such electrode results in the accumulation of hydroperoxide anions eq. (12) and consequehtly in the formation of $HO^{\bullet}$ and $HO_2^{\bullet}$ radicals by eqs. (13) and '(14). Metal peroxide compounds formed by eq. (13) remain stable at the potentials values ca. 0.70 V. This is supported by the experimental results of Markovic et. al.[38], who established that HO_2^{-} could be detected at the Au (100) ring electrode only at potentials below 0.716 V (RHE). The catalytic oxidation of hydroxyl compounds is described by eqs. (16) and (18) as illustrated by data in Figures 2 and 3.
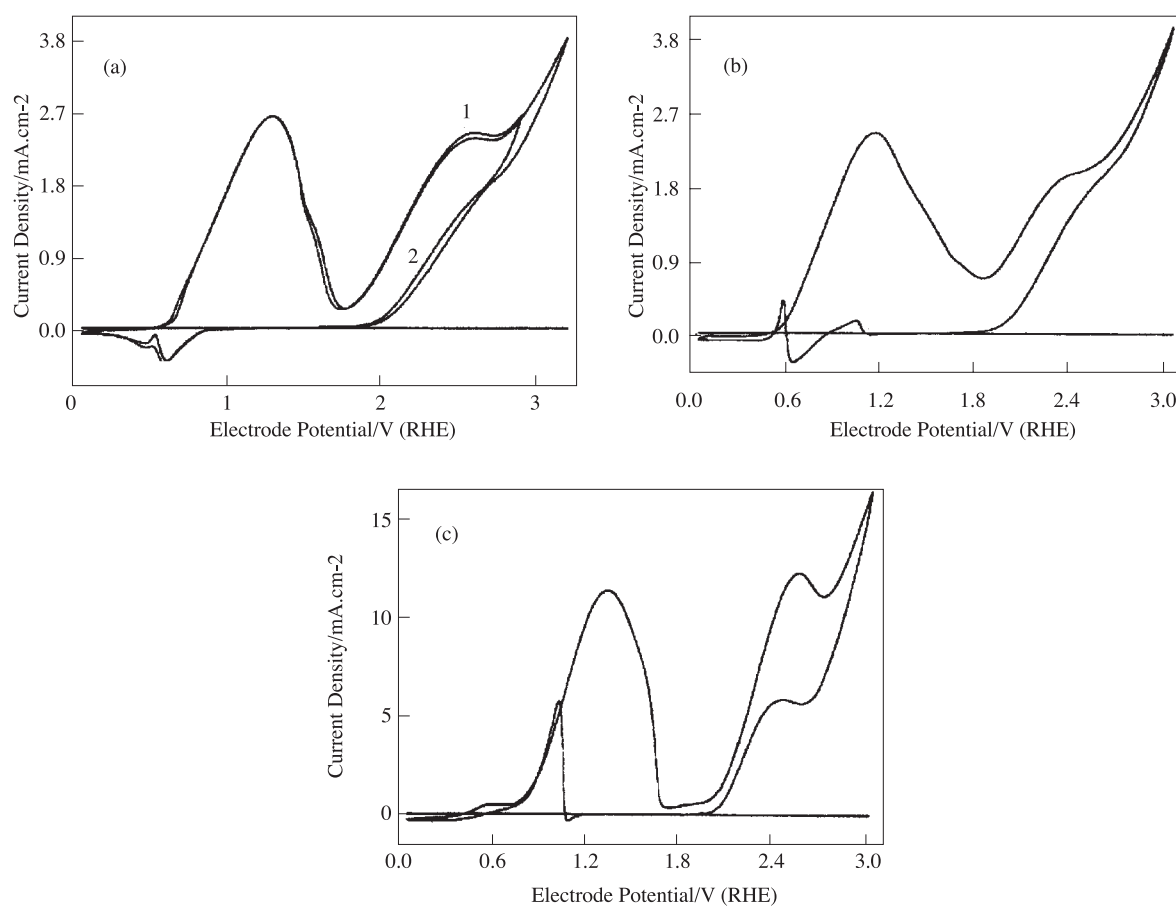

Figure 4. Effect of the upper potential limit on the reproducible potentiodynamic profiles recorded with a rate of 0.10 V.s^{-1} at 308.15 K in a solution containing 0.05 M KOH and 0.1 M glycerol at: (a) Pt:1-upper potential limit 2.90 V and 2-upper potential limit of 3.20 V; (b) Pt/Au (surface content of α_2-phase: 2.5 %); upper potential limit 3.05 V; (c) Au: upper potential limit 3.05.

In the absence of pre-oxidation of the catalytic surface the observed current densities are higher at Pt and lower at Au ant the alloy when referred to the corresponding preoxidized surfaces, as seen from Figures 3 and 4. The comparison of curves shown in Figure 3 (a) with that in Figure 4 (a) demonstrates that the observed current densities tend to increase with time approaching the value typical for the bare Pt surface. The behavior of Au is contrary to the described above, as the observed rates decrease with time tending to reach the limiting value typical for the unoxidized Au- surface. The alloy electrode behaves as an

intermadiate electrode resembling the properties of its consitituents, but is closer to that of Au.
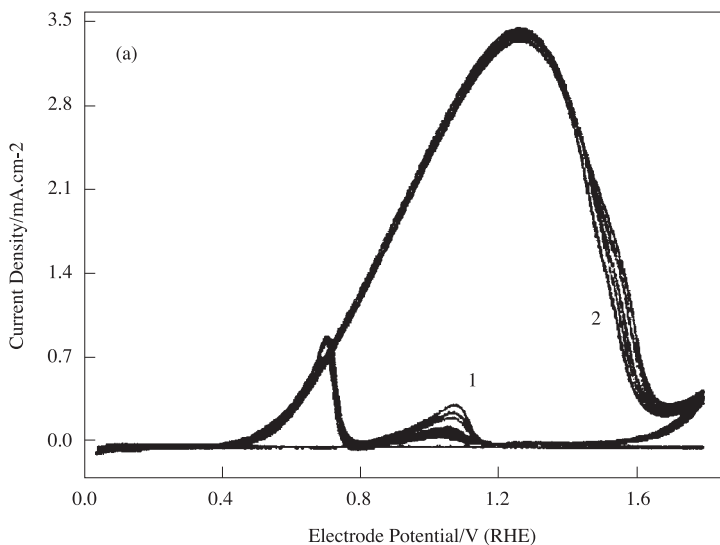
Figure 5a. Effect of Au adatoms on the subsequent potentiodynamic profiles recorded at Pt in the potential range 0.05-1.80 V with a rate 0.10 $V.s^{-1}$ at 308.25 K in a solution containing 0.05 M KOH and 0.1 M glycerol: 1-first profile; 2-tenth profile.
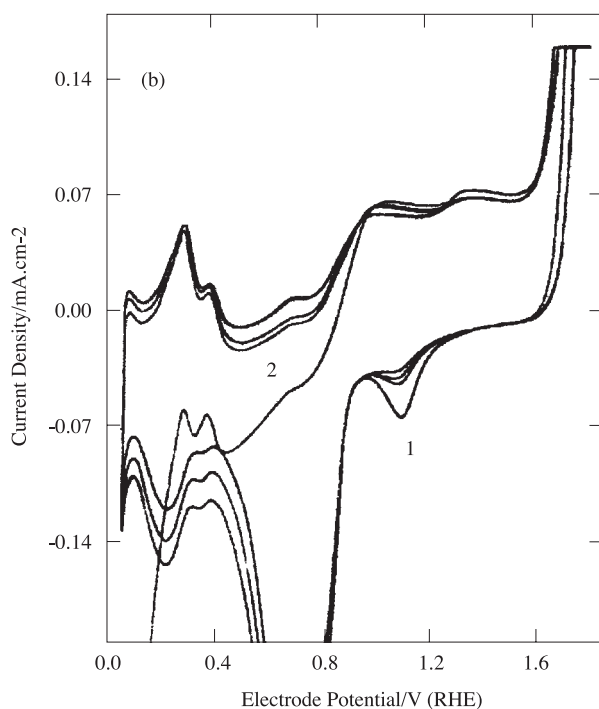
Figure 5b. Effect of Au adatoms on the subsequent potentiodynamic profiles recorded at Pt in the potential range 0.05-1.80 V with a rate of 0.10 $V.s^{-1}$ at 308.25 K in a solution containing 0.05 M KOH: 1- reproducible profile; 2-recorded after preliminary anodization for 20 s at 1.80 v in 0.05 M KOH. *Au adatoms were deposited on the surface of Pt through cathodic reduction of Au ions dissolved in 0.05 M KOH solution during the preliminary anodic dissolution of Au-oxides.

The catalytic behavior featured above could explained if the dissolution phenomena are taken into be accound as gold oxides are dissolved more rapidly compared with Pt -oxides which show an anomalous stability. During the dissolution process conditions are created allowing for the reposition of ions on the preoxidized electrode surface and thus permit the participation of the redox mediator system in the oxidative process. The present investigation relied exclusively on cyclic voltammetry which provides no data related to the composition and structure of the deposited films. In this connection the application of other techniques such as ellisometry and quartz crystal microbalance could provide the necessary information.

Acknowledgement

References

1. S. Trasatti, Int. J. Hydrogen Energy, 20, 835-844, (1995).

2. D. C. Johnson, N. Popovic, J. Feng, L. L. Houk and K. T. Kawagoe, Proc.-Electrochem. Soc., 95-26, 176-188, (1996)

3. C. Comninellis and A. De Battisti, J. Chim. Phys. 93, 673-679, (1996).

4. P. C. Lacaze, S. Hara, P. Soubrian and S. Aeiyach, Synth. Met. 76, 111-118, (1995).

5. P. I. Iotov and S. V. Kalcheva, J. Electroanal. Chem. 442, 19-26, (1998).

6. P. I. Iotov and S. V. Kalcheva, Bull. Electrochem. 15, 28-33 (1999).

7. P. I. Iotov and S. V. Kalcheva, J. Electroanal. Chem. (1999), submitted.

8. J. Lipkowski and L. Stolberg, in "Adsorption of Molecules at Metal Electrodes, (edited by J. Lipkowski and P. N. Ross), New York, VCH, 1992.

9. S. Trasatti, J. Electroanal. Chem. 54, 19-24 (1974).

10. M. Beltowska - Brzezinska, T. Luczak and R. Holze, J. Appl. Electrochem. 27, 999-1011, (1997), and references therein.

11. J. E. Vitt, L. A. Larew and D. C. Johnson, Electroanalysis, 2, 21-30, (1990).

12. M. Avramov-Ivic, M. Leger, C. Lamy, V. D. Jovic and S. D. Petrovic, J. Eletroanal. Chem., 308, 309-317, (1991).

13. B. Beden, J. M. Leger and C. Lamy, in Modern Aspects of Electrochem., 22, 97-264, (1992).

14. S. G. Sun, D. F. Yang and Z. W. Tian, Huaxue Xuebao, 50, 533-538, (1992).

15. G. Yildiz and F. Kadirgan, J. Electrochem. Soc. 141, 725-730, (1994).

16. M. Avramov-Ivic, V. Jovanovic, G. Vlajnic and J. Popic, J. Electroanal. Chem. 423, 119-124, (1997).

17. J. Heitbaum, Zwischenprodukte bei Elektrochemischen Reaktionen, Habilitationsschrift, Reinischen Friedrich-Wilhelms Universitat, Bonn, Oktober, 1977, p. 50.

18. L. D. Burke and G. P. Hopkins, J. Appl. Electrochem. 14, 679-686, (1984).

19. B. E. Conway, G. Tremilliosi-Filho and G. Jerkiewicz, J. Electroanal. Chem. 297, 435-443, (1991).

20. L. D. Burke and K. J. O'Dwyer, Electrochim. Acta, 37, 43-50, (1992).

21. G. Tremiliosi-Filho, L. H. Dall'Antonia and G. Jerkiewicz, J. Electroanal. Chem. 422, 149-159, (1997).

22. G. Jerkiewicz in A. Wieckowski (Ed.), Interfacial Electrochemistry, M. Decker, New York. 1998.

23. G. Jerkiewicz, J. J. Borodzinski, W. Chrzanowski and B. E. Conway, J. Electrochem. Soc. 142, 3755-3763, (1995).

24. C. C. Hu and T. C. Wen, J. Electrochem. Soc. 142, 1376-1383, (1995).

25. L. D. Burke and V. J. Cunnane, J. Electrochem. Soc. 133, 1657-1660, (1986).

26. L. D. Burke and W. A. O'Leary, J. Appl. Electrochem. 19, 758-767, (1989).

27. L. D. Burke, J. F. Healy, K. J. O'Dwyer and W. A. O'Leary, J. Electrochem. Soc. 136, 1015-1021, (1989).

28. L. D. Burke, V. J. Cunnane and B. H. Lee, J. Electrochem. Soc. 139, 399-406, (1992).

29. L. D. Burke, Platinum Metals Rev., 38, 166-173, (1994).

30. L. D. Burke and P. F. Nugent, Gold Bulletin, 30, 43-53, (1997).

31. L. D. Burke and P. F. Nugent, Gold Bulletin, 31, 39-51, (1998).

32. S. H. Cadle and S. Bruckenstein, Anal. Chem. 46, 16-20, (1974).

33. K. Juodkazis, J. Juodkazyte, T. Juodiene and A. Lukiskas, J. Electroanal. Chem. 441, 19-24, (1998).

34. B. E. Conway, H. Angerstein-Kozlowska, B. MacDougall and B. Tilak, in Theoretical and Experimental Study of Electrocatalysis and Application to the Oxidation of Hydrogen in an Acid Medium, Jurness Int. Etud. Piles Combust. C.R. 3-rd, eds. G. Feuillad et.al, pp. 163-170, Presses Acad. Eur. Brussels, Belgium, 1971.

35. R. Kotz and E. Yeager, J. Electroanal. Chem., 111, 105-110, (1980).

36. M. Fleischmann, I. R. Hill, G. Mengoli and M. M. Musiani, Electrochim. Acta 28, 1545-15553, (1983).

37. J. P. Hoare, J. Electrochem. Soc. 132, 301-306, (1985).

38. N. M. Markovic, I. M. Tidswell and P. N. Ross, Langmuir, 10, 1-4, (1994).

39. L. D. Burke and D. T. Buckley, J. Electroanal. Chem. 366, 239-251, (1994).

40. L. D. Burke and K. J. O'Dwyer, Electrochim. Acta, 37, 43-50, (1992).